Hierarchically Ordered Nanocomposites Self-Assembled from Linear-Alternating Block Copolymer/Nanoparticle Mixture

Liangshun Zhang and Jiaping Lin*

Key Laboratory for Ultrafine Materials of Ministry of Education, School of Materials Science and Engineering, East China University of Science and Technology, Shanghai 200237, China

Received November 12, 2008
Revised Manuscript Received January 2, 2009

ABSTRACT: Using self-consistent field and density functional theories, we undertake a first investigation on the hierarchically ordered structures self-assembled from linear-alternating block copolymer/nanoparticle mixture. The linear-alternating block copolymers self-assemble into the lamellar structure with two length scales, providing a template to direct the nanoparticle distribution. The spontaneously hierarchical organization of nanoparticles within the ordered copolymer structures was found to be dependent on the particle concentration and particle radius. Furthermore, the presence of the nanoparticles can also induce the hierarchical structure change due to the entropic effects. We envisage that this approach opens a gateway to construct hierarchically ordered nanocomposites with different length scales.

Introduction

Organization of inorganic nanoparticles within the self-assembled organic or biological templates provides new opportunities for the development of functional hydrid materials with enhanced optical, electrical and mechanical properties. In particular, dispersion of the nanoparticles into the diblock copolymer matrix has attracted considerable attraction because the ordered microstructures formed by the diblock copolymers can serve as templates to control the spatial arrangement of nanoparticles and thereby tailor the properties of the materials.[1−5] A challenge for further studies is to create hierarchically ordered nanocomposites inspired by the biological systems,[6−9] such as those found in the abalone nacre or mother of pearl. In these natural composites, the properties are an integrated consequence of assembled structures with various length scales. Essential to meeting the challenge is to construct a structural hierarchical matrix, which can provide templates for dispersion of nanoscopic elements.

The complex superstructures involving multiple length scales are found in the complicated copolymer architectures. For example, Ikkala, ten Brinke, and co-workers reported a hierarchical two-length-scale structure-within-structure self-assembled from a mixture containing a block copolymer and low molecular weight compound.[10,11] In such a system, the block copolymer and the low molecular weight compound can be weakly connected by hydrogen bonds. The large-length-scale lamella is formed by the block copolymers, while the short-length-scale lamella is formed by the bound low molecular weight compound. Another possibility to produce the hierarchical structure is to take advantage of $\mathbf{A}_m$-*b*-(**B**-*b*-**A**)$_n$ linear-alternating block copolymer, which is a drastic simplification of the above mixture system. The repeat unit of the hierarchical structure formed by the linear-alternating copolymers is composed of one thick A layer and several thin A and B layers.[12−15] When the nanoparticles are incorporated into the linear-alternating block copolymers, this structure is expected to promote the formation of hierarchically ordered nanocomposites in one effective step and thereby tailors the properties of materials. The novel hierarchical structures may provide new opportunities for designing the nanocomposites with controllable properties and multifunctionality.

A recent numerical approach developed by Balazs and co-workers has addressed the polymer nanoparticle composites by coupling the self-consistent field theory (SCFT) for polymers and density functional theory (DFT) for particles.[16−22] SCFT is used to characterize the equilibrium thermodynamic features of polymer system,[23−25] while DFT captures the behavior of particle ordering.[26] The integrated SCFT/DFT technique identifies new self-assembly morphologies of the blend of diblock copolymers and nanoparticles, where the particles and copolymers can organize into mesoscopically regular patterns. A powerful feature of this method is that priori assumptions about the morphology and the distribution of particles are not necessary. Balazs et al. found that the morphologies of diblock copolymers and distributions of particles can be tailored by the concentration of adding particles, the size of particles, the interaction between the particles and blocks, and the polydispersity of particles. In our previous work, we utilized SCFT/DFT methodology to investigate the self-assembly behavior of amphiphilic block copolymer/nanoparticle mixture in dilute solution.[22] The mixture can self-associate into microstructures with controllable size and morphology in selective solvent and the nanoparticles are spatially organized into the microstructures.

In this study, we present a first example, to the best of our knowledge, of hierarchically ordered nanocomposite self-assembled from linear-alternating block copolymers and nanoparticles. The SCFT/DFT method was applied to investigate the cooperative behavior and novel structures where the nanoparticles are incorporated into the linear-alternating copolymers. It was found that the linear-alternating copolymers can self-assemble into the hierarchical lamellar structure with two length scales. When the nanoparticles are introduced, the nanoparticles and copolymers spontaneously order into a hierarchical regular structure. Furthermore, the incorporated nanoparticles can also induce the change of hierarchical structure.

Theoretical Model

We consider a system with volume V containing a mixture of molten linear-alternating block copolymers and solid spherical particles. All particles have the same radius R_P. The overall concentration of particles in the system, expressed in volume fraction, is Ψ_P. The linear-alternating block copolymers, denoted as $\mathbf{A}_m$-*b*-(**B**-*b*-**A**)$_n$, consist of a long homopolymer $\mathbf{A}_m$ block connected to a (**B**-*b*-**A**)$_n$ multiblock of n identical diblock repeat units (see Figure 1a). The volume fraction of long homopolymer $\mathbf{A}_m$ block per chain is denoted by f. Each chain is modeled as a flexible Gaussian chain consisting of N segments of segment volume $\rho_0^{-1}$and statistical segment length a.

According to SCFT/DFT, the free energy F for the present system is written as

* Corresponding author. Telephone: +86-21-64253370. Fax: +86-21-64253539. E-mail: jplinlab@online.sh.cn.

10.1021/ma802539q CCC: $40.75
Published on Web 01/29/2009

$$\frac{NF}{\rho_0 k_B TV} = -(1-\psi_P)\ln\left(\frac{Q_C}{V(1-\psi_P)}\right) - \frac{\psi_P}{\alpha}\ln\left(\frac{Q_P\alpha}{V\psi_P}\right) + \frac{1}{V}\int d\mathbf{r}\left[\frac{1}{2}\sum_{\mu,\nu=A,B,P;\mu\neq\nu}\chi_{\mu\nu}N\varphi_\mu(\mathbf{r})\varphi_\nu(\mathbf{r}) - \sum_{\mu=A,B}\omega_\mu(\mathbf{r})\varphi_\mu(\mathbf{r}) - \omega_P(\mathbf{r})\rho_P(\mathbf{r})\right] + \frac{1}{V}\int d\mathbf{r}\ \rho_P(\mathbf{r})\Psi_{HS}(\bar{\varphi}_P(\mathbf{r})) \quad (1)$$

Here, k_B is Boltzmann's constant and T is the temperature. α is the volume ratio of the particle with radius R_P to linear-alternating block copolymer chain. χ_{IJ} characterizes the interaction between species I and J. Self-consistent fields given by $\omega_A(\mathbf{r})$, $\omega_B(\mathbf{r})$, and $\omega_P(\mathbf{r})$ account for the average interactions, which act on the A and B segments of copolymers and the particles, respectively. $\phi_A(\mathbf{r})$, $\phi_B(\mathbf{r})$ and $\phi_P(\mathbf{r})$ are the local volume fractions of A-segment, B-segment, and particles, respectively. $\rho_P(\mathbf{r})$ is the center distribution of particles. The local particle volume fraction $\phi_P(\mathbf{r})$ is related to particle center distribution $\rho_P(\mathbf{r})$ by $\phi_P(\mathbf{r}) = (3\alpha)/(4\pi R_P^3)\int_{|\mathbf{r}'|<R_P} d\mathbf{r}'\ \rho_P(\mathbf{r}+\mathbf{r}')$. Q_P is the partition function for single particle under the self-consistent field $\omega_P(\mathbf{r})$ given by $Q_P = \int d\mathbf{r}\ \exp(-\omega_P(\mathbf{r}))$. $Q_C = \int d\mathbf{r}\ \mathbf{q}(\mathbf{r},s)q^+(\mathbf{r},1-s)$ is the partition function for single linear-alternating block copolymer subject to the $\omega_A(\mathbf{r})$ and $\omega_B(\mathbf{r})$ fields. The contour length s increases continuously from 0 to 1 as the segment changes from one end to the other. The spatial coordinate $\mathbf{r}$ is in units of R_g ($R_g^2 = N^2a/6$). The propagator $q(\mathbf{r}, s)$ represents the probability of finding segments sN at position $\mathbf{r}$, which satisfies the modified diffusion equation

$$\frac{\partial q(\mathbf{r},s)}{\partial s} = \nabla^2 q(\mathbf{r},s) - \omega(\mathbf{r})q(\mathbf{r},s) \quad (2)$$

subject to the initial condition $q(\mathbf{r},0) = 1$ and with $\omega(\mathbf{r},s) = \sum_\alpha \sigma_\alpha \omega_\alpha(\mathbf{r})$ (α = A, B). Here, σ_α defines the architecture of copolymers; i.e., this function is unity if segment sN is of type α and zero otherwise. Similarly, the backward propagator $q^+(\mathbf{r},s)$ is defined. The last term of eq 1 describes the steric free energy of the particles according to Carnahan−Starling function $\Psi_{HS}(x) = (4x - 3x^2)/((1-x)^2)$.[27] $\bar{\phi}_P(\mathbf{r})$ is the weighted nonlocal volume fraction of particles. The relationship between $\bar{\phi}_P(\mathbf{r})$ and $\rho_P(\mathbf{r})$ is as follows: $\bar{\phi}_P(\mathbf{r}) = (\alpha/v_{2R_P})\int_{|\mathbf{r}'|<2R_P} d\mathbf{r}'\ \rho_P(\mathbf{r}+\mathbf{r}')$, where v_{2R_P} is the volume of a sphere with radius $2R_P$.

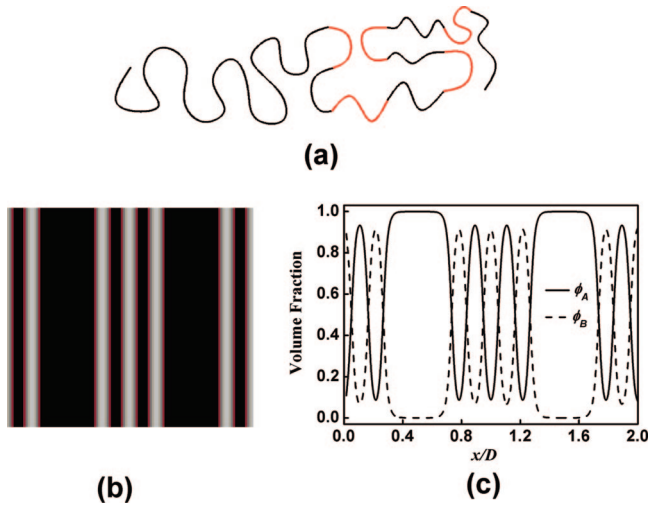

Figure 1. (a) Schematic representation of $\mathbf{A}_m$-*b*-($\mathbf{B}$-*b*-$\mathbf{A}$)$_n$ linear-alternating block copolymer. (b) Two-dimensional density profile of A-type segment in linear-alternating copolymer melt for $f = 0.40$ and $n = 5$ at $\chi_{AB}N = 200.0$. Light gray regions represent lower local volume fraction of A-type segment, while black regions represent higher local volume fraction of A-type segment. (c) Distribution profiles of A- and B-type segments along the line normal to the lamella. The spatial coordinate x is expressed in units of the domain spacing D.

More details about the SCFT/DFT for the polymer/nanoparticle system can be found in previous studies.[17,22]

Equation 1 determines the free energy of the system as a function of the local densities ($\phi_A(\mathbf{r})$, $\phi_B(\mathbf{r})$, and $\rho_P(\mathbf{r})$) and local chemical potential fields ($\omega_A(\mathbf{r})$, $\omega_B(\mathbf{r})$, and $\omega_P(\mathbf{r})$). By minimizing the free energy of eq 1 with respect to fields and densities, we obtain a set of self-consistent equations describing the microstructures of linear-alternating copolymer/nanoparticle composites subject to the incompressibility constraint ($\phi_A(\mathbf{r}) + \phi_B(\mathbf{r}) + \phi_P(\mathbf{r}) = 1$):

$$\omega_A(\mathbf{r}) = \chi_{AB}N\varphi_B(\mathbf{r}) + \chi_{AP}N\varphi_P(\mathbf{r}) \quad (3)$$

$$\omega_B(\mathbf{r}) = \chi_{AB}N\varphi_A(\mathbf{r}) + \chi_{BP}N\varphi_P(\mathbf{r}) \quad (4)$$

$$\omega_P(\mathbf{r}) = \Psi_{HS}(\overline{\varphi_P}(\mathbf{r})) + \frac{a}{v_{2R_P}}\int_{|\mathbf{r}'|<2R_P} d\mathbf{r}'\ \rho_P(\mathbf{r}+\mathbf{r}')\Psi'_{HS}(\overline{\varphi_P}(\mathbf{r}+\mathbf{r}')) + \frac{a}{v_{R_P}}\int_{|r'|<R_P} d\mathbf{r}'\ [x_{AP}N\varphi_A(\mathbf{r}+\mathbf{r}') + x_{BP}N\varphi_B(\mathbf{r}+\mathbf{r}')] \quad (5)$$

where $\Psi'_{HS}(x) = d\Psi_{HS}(x)/dx$

$$\varphi_A(\mathbf{r}) = \frac{V(1-\psi_P)}{Q_C}\int_0^1 ds\ q(\mathbf{r},s)q^+(\mathbf{r},1-s)\sigma_A(s) \quad (6)$$

$$\varphi_B(\mathbf{r}) = \frac{V(1-\psi_P)}{Q_C}\int_0^1 ds\ q(\mathbf{r},s)q^+(\mathbf{r},1-s)\sigma_B(s) \quad (7)$$

$$\rho_P(\mathbf{r}) = \frac{V\psi_P}{Q_P\alpha}\exp(-\omega_P(\mathbf{r})) \quad (8)$$

The resulting equations were solved numerically by the real-space combinational screening algorithm in two-dimensions at strong segregation strength developed Fredrickson et al.[28,29] We discretized both the spatial and the contour coordinates and used an unconditionally stable backward differentiation formula method to solve the modified diffusion equation for system with sharp interfaces. For example, the modified diffusion equation Eq.(2) was discretized according to

$$\frac{25}{12}q_{n+1} - 4q_n + 3q_{n-1} - \frac{4}{3}q_{n-2} + \frac{1}{4}q_{n-3} = \Delta s[\nabla^2 q_{n+1} - \omega(4q_n - 6q_{n-1} + 4q_{n-2} - q_{n-3})] \quad (9)$$

Here, q_{n+i} denotes $q(\mathbf{r}, s+i\Delta s)$ and Δs is the step size. We employed the Anderson mixing method to solve the self-consistent equations.[30] Having a solution of SCFT equations, one can calculate the free energy. Free energy minimization of the system with respect to the selected simulation box size was performed in the calculations.[31]

Results and Discussion

We begin by considering a typical example where the linear-alternating copolymers self-assemble into the hierarchically ordered structures. We set $f = 0.40$ and $n = 5$, where the long homopolymer $\mathbf{A}_m$ block and the ($\mathbf{B}$-*b*-$\mathbf{A}$)$_n$ multiblock can form the lamellar structure above the order−disorder transition. We also set $\chi_{AB}N = 200.0$, which is sufficient to produce the microphase separation of ($\mathbf{B}$-*b*-$\mathbf{A}$)$_5$ multiblock, resulting in a lamellar-within-lamellar structure. Figure 1b shows the two-dimensional density profile of A-blocks. The morphology of the system is lamella-within-lamella. Figure 1c is the density distribution profiles of A and B segments along the line normal to the lamella. As can be seen, the linear-alternating block copolymers form the large-length-scale lamella. Meanwhile, the microphase separation of ($\mathbf{B}$-*b*-$\mathbf{A}$)$_5$ multiblock occurs and five thinner layers are formed within the large-length-scale lamella.

When the nanoparticles are incorporated into the linear-alternating copolymer melts, the lamellar-within-lamellar struc-

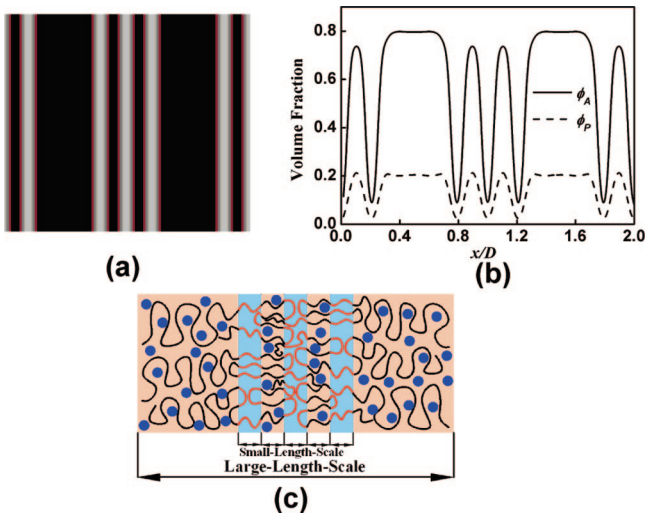

Figure 2. (a) Two-dimensional density profile of nanoparticles for linear-alternating copolymer/nanoparticle system obtained from the SCFT/DFT approach. The parameters are $f = 0.40$, $n = 5$, $\chi_{AB}N = 200.0$, $\chi_{AP}N = 0.0$, $\chi_{BP}N = 200.0$, R_P=0.20R_g, and Ψ_P=0.15. The nanoparticles are distributed in the A-domains of large-length-scale layer and small-length-scale layers. Light gray regions represent lower local volume fraction of particles, while black regions represent higher local volume fraction of particles. (b) Distribution profiles of A-type segments and nanoparticles along the line normal to lamella. (c) Schematic representation of the nanoparticle arrangement in the lamellar-within-lamellar structure formed by the linear-alternating copolymers. The black lines, red lines, and circles filled with blue color denote the A-type blocks, B-type blocks, and nanoparticles, respectively.

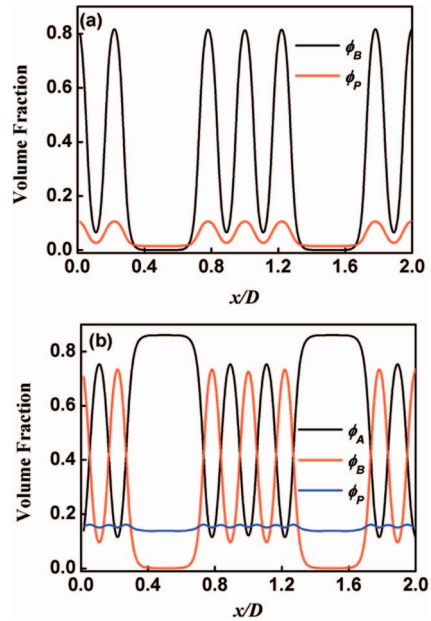

Figure 3. (a) Distribution profiles of B-type segments and nanoparticles along the line normal to lamella. The parameters are $f = 0.40$, $n = 5$, $\chi_{AB}N = 200.0$, $\chi_{AP}N = 200.0$, $\chi_{BP}N = 0.0$, $R_P = 0.15R_g$, and $\Psi_P = 0.05$. In this case, the particles are preferential to B blocks. (b) Distribution profiles of A-type segments, B-type segments, and nanoparticles along the line normal to lamella. The parameters are $f = 0.40$, $n = 5$, $\chi_{AB}N = 200.0$, $\chi_{AP}N = 0.0$, $\chi_{BP}N = 0.0$, $R_P = 0.15R_g$, and $\Psi_P = 0.15$. In this scenario, the particles are not selective to the A and B blocks.

ture serves as a template to direct distribution of the nanoparticles within different length scales. With the above parameters fixed, we now introduce a volume fraction $\Psi_P = 0.15$ of selective particles characterized by $\chi_{AP}N = 0.0$, $\chi_{BP}N = 200.0$, and $R_P = 0.20R_g$, where R_g is the ideal gyration radius of linear-alternating copolymer. This causes the particles to be preferentially localized in the A-domains. The density profiles are shown in Figure 2a and 2b. The entire system is organized into well-ordered structure and the nanoparticles are accommodated in the **A**-domains of both large and small-length-scale layers. The nanoparticle distribution in the linear-alternating copolymer/nanoparticle system reveals a new structural feature. As shown in Figure 2b, the repeat unit of the pattern consists of one thick nanoparticle layer and two thin nanoparticle layers. Thus, a synchronized structure with double periodicities is spontaneously formed in the present system. The organization of the nanoparticles in the linear-alternating copolymers is schemed in Figure 2c. The linear-alternating block copolymers self-assemble into the large-length-scale lamella and multiblock part of copolymers form the five small-length-scale layers in a repeat unit. The nanoparticles are distributed into A-domain with different length scales due to the affinity between the particles and A-blocks.

We also examined the influence of the selectivity of the nanoparticles on the formed microstructures. In addition to A block selectiveness, the nanoparticles with B block selectiveness and nonselectiveness are considered. The density distributions of B blocks and nanoparticles with B block selectiveness are shown in Figure 3a. As the nanoparticles are selective to B blocks, the nanoparticles are only distributed into the small-length-scale lamellas. For the nonselective nanoparticles, the density distributions of A blocks, B blocks, and neutral nanoparticles are illustrated in Figure 3b. The nonselective nanoparticles are almost uniformly distributed into the all length scale lamellas. It is noted that a slight interfacial segregation of nonselective nanoparticles occurs in the small-length-scale lamellas. Such segregation could contribute to the reduction of the interface energy between A and B blocks. From above results, we learned that the hierarchically ordered nanocomposites can be formed only when the nanoparticles are selective to the A blocks.

To achieve further understanding of the hierarchical behavior of linear-alternating copolymer/nanoparticle composite, density fields at various particle radii and particle concentrations were calculated for copolymer/A block selective nanoparticle system (Figure 4). As shown in Figure 4a, small selective nanoparticles are distributed in both large- and small-length-scale lamellas. When the nanoparticles diameter is larger than the thickness of small-length-scale layers, the nanoparticles are not lodged in the small-length-scale layers. It is also noted that variation of nanoparticle concentration can change the number of thin layers in a repeat unit. As shown in Figure 4b, there is only one maximum for the nanoparticle distribution of the small-length-scale layer within the large-length-scale lamella when Ψ_P is larger than 0.1, indicating that the number of small-length-scale layers changes from five to three.

The difference of nanoparticle distribution in the hierarchical structure can be rationalized by considering the entropic contribution from polymer chains and particles. The size ratio of homopolymer $\mathbf{A}_m$ blocks to particles is much larger than that of A blocks of $(\mathbf{B}\text{-}b\text{-}\mathbf{A})_5$ multiblocks to particles. Thus, the configurational entropic contribution of linear-alternating chains comes mainly from the strongly stretching of A blocks of $(\mathbf{B}\text{-}b\text{-}\mathbf{A})_5$ multiblocks around the nanoparticles. This significantly affects the nanoparticle distribution within the small-length-scale layer and the structure of small-length-scale layer. As the nanoparticle radius or concentration increases, A blocks of $(\mathbf{B}\text{-}b\text{-}\mathbf{A})_5$ multiblocks tend to be stretched, resulting in an increase in free energy. To alleviate this effect, the stretching of A blocks of $(\mathbf{B}\text{-}b\text{-}\mathbf{A})_5$ multiblocks is reduced by the segregation of

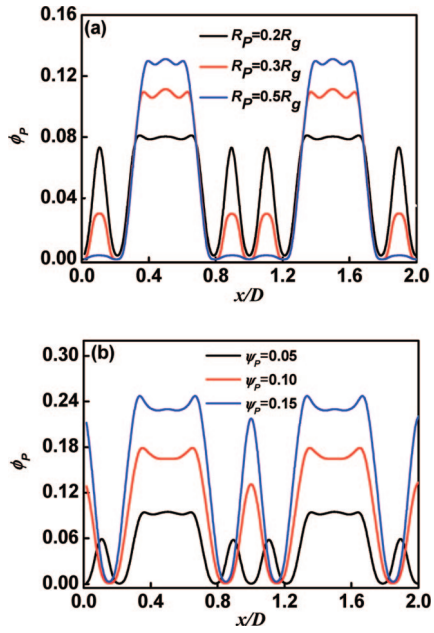

Figure 4. (a) Distribution profiles of nanoparticles along the line normal to the lamella with various particle radii for $\Psi_P = 0.05$. (b) Distribution profiles of nanoparticles along the line normal to the lamella with various particle concentrations at $R_P = 0.25R_g$. The other parameters are the same as in Figure 2.

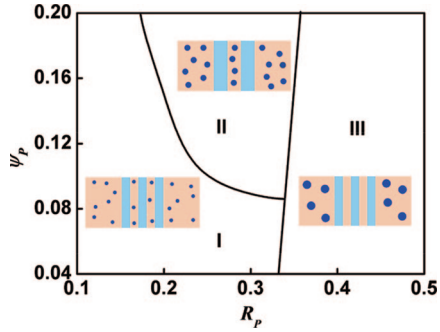

Figure 5. Nanoparticle distribution in the lamellar-within-lamellar structure for a range of nanoparticle radii R_P and nanoparticle concentrations Ψ_P. In region I, the nanoparticles are distributed into the large-length-scale layer and two small-length-scale layers in a repeat unit. In region II, the nanoparticles are distributed into the large-length-scale layer and one small-length-scale layer. In region III, the nanoparticles only exist in the large-length-scale lamella.

particles into the large-length-scale lamella (Figure 4a) or by decreasing the number of small-length-scale layers to reduce the lodged volume fraction of particles in small-length-scale layers (Figure 4b). As a result, the particles in small-length-scale layers and the number of small-length-scale layers change with increasing nanoparticle radius or concentration.

To qualitatively understand the dependence of nanoparticle distribution in linear-alternating copolymers on the particle size and particle concentration, we carried out several simulations for various particle radii and particle volume fractions. The results of these simulations are summarized into a phase diagram as shown in Figure 5. As can be seen, the nanoparticles are distributed in one thick layer and two thin layers when the nanoparticle radius and concentration are small (region I). As the particle radius and concentration increase, the number of thin layers in a repeat unit becomes three due to the entropic penalty associated with the stretching of A blocks of $(\mathbf{B}\text{-}b\text{-}\mathbf{A})_5$ multiblocks and the nanoparticles are distributed into one thick layer and one thin layer (region II). In particular, when the size of nanoparticles is large enough, the nanoparticles are only found in the large-length-scale lamella (region III). It was recently reported that nanoparticles can induce transitions between various phases formed by parent block copolymers.[32−35] For example, Kramer et al. reported that the presence of nanoparticles can force the lamellar phase of diblock copolymer into cylindrical phase.[33] For the linear-alternating copolymers considered in the present work, when the architectures of copolymers (e.g., the volume fraction of A block and asymmetry of multiblock) change, other complex hierarchical structures such as cylinder-within-lamella and lamella-within-cylinder might be formed. Under such circumstances, the nanoparticles may induce phase transitions between these different phases as reported in literature, and more complicated phase behaviors can be exhibited.

For the well-studied diblock copolymer/nanoparticle mixture,[2,16] the microphase separation of diblock copolymers can only form the one-length-scale ordered structures, which direct the spatial distribution of nanoparticles. As shown above, replacing the diblock copolymers with the linear-alternating copolymers creates a multiple-length-scale particle distribution within the structure-in-structure domain. The system is hierarchically ordered nanocomposite as a result of the self-directed assembly of nanoparticle and linear-alternating copolymer mixture. If the particles exhibit unique properties, each scale layer can contribute a distinct function to yield an integrated and multifunctional material like the natural organic/inorganic composites of bone and abalone nacre.

In summary, we report here an example of hierarchical ordered nanocomposites, which is generated by self-directed assembly of nanoparticle and linear-alternating copolymer mixture. Depending on the nanoparticle concentration and nanoparticle radius, the nanoparticles are distributed in the different length scale lamellas. The results may provide a useful guide for fabricating functional nanocomposites in the field of material design and understanding the hierarchical self-assembly behavior in nature. The approach is also helpful for understanding the hierarchical distribution of nanoparticles in other architecture copolymers, such as the comb-shaped supramolecules, which can form the more complicated lamellar-within-cylindrical, cylindrical-within-lamellar structures.

Acknowledgment. This work was supported by the National Natural Science Foundation of China (50673026, 20574018). Support from Doctoral Foundation of Education Ministry of China (Grant No. 20050251008) and Projects of Shanghai Municipality (06SU07002, 0652nm021, 082231, and B502) are also appreciated.

References and Notes

(1) Balazs, A. C.; Emrick, T.; Russell, T. P. *Science* **2006**, *314*, 1107.
(2) Lin, Y.; Boker, A.; He, J.; Sill, K.; Xiang, H.; Abetz, C.; Li, X.; Wang, J.; Emrick, T.; Long, S.; Wang, Q.; Balazs, A. C.; Russell, T. P. *Nature* **2005**, *434*, 55.
(3) Hamley, I. W. *Angew. Chem., Int. Ed.* **2003**, *42*, 1692.
(4) Blockstaller, M. R.; Mickiewiez, R. A.; Thomas, E. L. *Adv. Mater.* **2005**, *17*, 1331.
(5) Kang, H.; Detcheverry, F. A.; Mangham, A. N.; Stoykovich, M. P.; Daoulas, K. Ch.; Hamers, R. J.; Muller, M.; dePablo, J. J.; Nealey, P. F. *Phys. Rev. Lett.* **2008**, *100*, 148303.
(6) Simon, P.; Schwarz, U.; Kniep, R. *J. Mater. Chem.* **2005**, *15*, 4992.
(7) Birnkrant, M. J.; Li, C. Y.; Natarajan, L. V.; Tondiglia, V. P.; Sutherland, R. L.; Lloyd, P. F.; Bunning, T. J. *Nano Lett.* **2007**, *7*, 3128.
(8) Wagner, H. D. *Nature Nanotech.* **2007**, *2*, 742.
(9) Vaia, R.; Baur, J. *Science* **2008**, *319*, 420.
(10) Ruokolainen, J.; Makinen, R.; Torkkeli, M.; Makela, T.; Serimaa, R.; ten Brinke, G.; Ikkala, O. *Science* **1998**, *280*, 557.
(11) Ikkala, O.; ten Brinke, G. *Science* **2002**, *295*, 2407.

(12) Masuda, J.; Takano, A.; Nagata, Y.; Noro, A.; Matsushita, Y. *Phys. Rev. Lett.* **2006**, *97*, 098301.
(13) Matsushita, Y. *Macromolecules* **2007**, *40*, 771.
(14) Nap, R.; Sushko, N.; Erukhimovich, I.; ten Brinke, G. *Macromolecules* **2006**, *39*, 6765.
(15) Subbotin, A.; Klymko, T.; ten Brinke, G. *Macromolecules* **2007**, *40*, 2915.
(16) Thompson, R. B.; Ginzburg, V. V.; Matsen, M. W.; Balazs, A. C. *Science* **2001**, *292*, 2469.
(17) Thompson, R. B.; Ginzburg, V. V.; Matsen, M. W.; Balazs, A. C. *Macromolecules* **2002**, *35*, 1060.
(18) Lee, J.-Y.; Thompson, R. B.; Jasnow, D.; Balazs, A. C. *Phys. Rev. Lett.* **2002**, *89*, 155503.
(19) Lee, J.-Y.; Shou, Z.; Balazs, A. C. *Phys. Rev. Lett.* **2003**, *91*, 136103.
(20) Spontak, R. J.; Shankar, R.; Bowman, M. K.; Krishnan, A. S.; Hamersky, M. W.; Samseth, J.; Bockstaller, M. R.; Rasmussen, K. O. *Nano Lett.* **2006**, *6*, 2115.
(21) Ginzburg, V. V.; Balijepalli, S. *Nano Lett.* **2007**, *7*, 3716.
(22) Zhang, L.; Lin, J.; Lin, S. *Macromolecules* **2007**, *40*, 5582.
(23) Matsen, M. W. *J. Phys.: Condens. Matter* **2002**, *14*, R21.
(24) Fredrickson, G. H. *The Equilibrium Theory of Inhomogeneous Polymers*; Oxford University Press: Oxford, U.K., 2006.
(25) Zhang, L.; Lin, J.; Lin, S. *J. Phys. Chem. B* **2007**, *111*, 351.
(26) Vroege, G. J.; Lekkerkerker, H. N. W. *Rep. Prog. Phys.* **1992**, *55*, 1241.
(27) Carnahan, N. F.; Starling, K. E. *J. Chem. Phys.* **1969**, *51*, 635.
(28) Drolet, F.; Fredrickson, G. H. *Phys. Rev. Lett.* **1999**, *83*, 4317.
(29) Cochran, E. W.; Garcia-Cervera, G. J.; Fredrickson, G. H. *Macromolecules* **2006**, *39*, 2449.
(30) Eyert, V. *J. Comput. Phys.* **1996**, *124*, 271.
(31) Bohbot-Raviv, Y.; Wang, Z.-G. *Phys. Rev. Lett.* **2000**, *85*, 3428.
(32) Chiu, J. J.; Kim, B. J.; Kramer, E. J.; Pine, D. J. *J. Am. Chem. Soc.* **2005**, *127*, 5036.
(33) Sides, S. W.; Kim, B. J.; Kramer, E. J.; Fredrickson, G. H. *Phys. Rev. Lett.* **2006**, *96*, 250601.
(34) Kim, B. J.; Chiu, J. J.; Yi, G.-R.; Pine, D. J.; Kramer, E. J. *Adv. Mater.* **2005**, *17*, 2618.
(35) Yeh, S.-W.; Wei, K.-H.; Sun, Y.-S.; Jeng, U.-S.; Liang, K. S. *Macromolecules* **2005**, *38*, 6559.

MA802539Q